

This article was downloaded by:

On: 25 January 2011

Access details: *Access Details: Free Access*

Publisher *Taylor & Francis*

Informa Ltd Registered in England and Wales Registered Number: 1072954 Registered office: Mortimer House, 37-41 Mortimer Street, London W1T 3JH, UK



## Liquid Crystals

Publication details, including instructions for authors and subscription information:

<http://www.informaworld.com/smpp/title~content=t713926090>

### Fast switching near a smectic-to-nematic phase transition

Sebastian Gauza<sup>a</sup>; Amanda Parish<sup>a</sup>; Shin-Tson Wu<sup>a</sup>; Anna Spadło<sup>b</sup>; Roman Dabrowski<sup>b</sup>

<sup>a</sup> College of Optics and Photonics, University of Central Florida, Orlando, USA <sup>b</sup> Institute of Chemistry, Military University of Technology, 00-908 Warsaw, Poland

**To cite this Article** Gauza, Sebastian , Parish, Amanda , Wu, Shin-Tson , Spadło, Anna and Dabrowski, Roman(2008) 'Fast switching near a smectic-to-nematic phase transition', *Liquid Crystals*, 35: 6, 711 – 717

**To link to this Article:** DOI: 10.1080/02678290802120299

**URL:** <http://dx.doi.org/10.1080/02678290802120299>

PLEASE SCROLL DOWN FOR ARTICLE

Full terms and conditions of use: <http://www.informaworld.com/terms-and-conditions-of-access.pdf>

This article may be used for research, teaching and private study purposes. Any substantial or systematic reproduction, re-distribution, re-selling, loan or sub-licensing, systematic supply or distribution in any form to anyone is expressly forbidden.

The publisher does not give any warranty express or implied or make any representation that the contents will be complete or accurate or up to date. The accuracy of any instructions, formulae and drug doses should be independently verified with primary sources. The publisher shall not be liable for any loss, actions, claims, proceedings, demand or costs or damages whatsoever or howsoever caused arising directly or indirectly in connection with or arising out of the use of this material.

## Fast switching near a smectic-to-nematic phase transition

Sebastian Gauza<sup>a\*</sup>, Amanda Parish<sup>a</sup>, Shin-Tson Wu<sup>a</sup>, Anna Spadło<sup>b</sup> and Roman Dabrowski<sup>b</sup>

<sup>a</sup>College of Optics and Photonics, University of Central Florida, Orlando, FL 32816, USA; <sup>b</sup>Institute of Chemistry, Military University of Technology, 00-908 Warsaw, Poland

(Received 5 March 2008; final form 10 April 2008)

We have designed, synthesised and evaluated the physical properties of high-birefringence ( $\Delta n$ ) isothiocyanato phenyl-tolane and terphenyl liquid crystals. These compounds exhibit a  $\Delta n \sim 0.36$ – $0.52$  at room temperature and wavelength  $\lambda = 633$  nm. A different mesomorphic sequence was observed depending on the terminal alkyl chain length. Compounds with a longer chain show smectic and nematic phases, whereas short-chain homologues only exhibit a nematic phase. In the vicinity of the nematic-to-smectic transition, the viscoelastic coefficient decreases, instead of increases, as the temperature decreases. The observed change is as large as 75% for the 4'-(3,5-difluoro-4-isothiocyanatophenylethynyl)-4-pentylbiphenyl compound studied. This behaviour is useful for improving the response time of a liquid crystal device, if the operating temperature can be controlled accurately.

**Keywords:** high birefringence; isothiocyanato phenyl-tolanes; smectic–nematic phase transition

### 1. Introduction

It is highly desirable that liquid crystal (LC) compounds and mixtures exhibit a wide range of mesomorphic phase depending on the specific application. Such a mesomorphic phase is achieved either by a single compound or by a eutectic mixture. Numerous reports have been published regarding binary or multicomponent LC systems that exhibit induced smectic A (specifically  $A_d$ ), re-entrant nematic and also ferroelectric and antiferroelectric phases (1–3). These induced phases are often attractive for phase transition boundary studies. The close proximity of the phase transition typically introduces unexpected deviations of the major physical properties, e.g. dielectric permittivity, elastic constants, flow viscosity or rotational viscosity, as the order parameter of the LC changes drastically (4–10). The phase transition between nematic phase (which has orientational order) and smectic phase (which has both orientational and positional orders) has long been studied for subtle effects that arise from the intrinsic coupling of their order parameters (11). To combine the typical nematic behaviour observed by different experimental techniques (polarising optical microscopy, miscibility studies and dielectric spectroscopy) and the smectic-like fluctuations (short-range positional order) in the systems with smectic and nematic phase, the term cybotactic nematic has been used. It is known from X-ray diffraction patterns that small domains with a local smectic organisation appear in the nematic phase just above the transition point, and the domains are cybotactic clusters (12).

Recently we have reported some new high-birefringence ( $\Delta n > 0.4$ ) single compounds (13–15) and formulated high-birefringence mixtures for laser beam steering and optical shutter applications (16–18). These applications require fast (millisecond) response time. In order to achieve fast response time, a straightforward approach is to employ a thin cell filled with a high-birefringence mixture and operated at an elevated temperature (19–21). To avoid ambient temperature fluctuations, the LC device is enclosed in a temperature-stabilised chamber. High-birefringence LCs are typically identified with long conjugated rigid cores linked with a highly polar group, e.g. cyano (CN). For instance, a structure like 5CB (pentylcyanobiphenyl) has a linear  $\pi$ -electron conjugation extending over the biphenyl rigid core and the polar terminal cyano group. As a result, its optical and dielectric anisotropies are relatively high.

Our research focuses on elongated molecular rigid cores, such as tolane, terphenyl and phenyl-tolane, with isothiocyanato (NCS) terminal polar group instead of cyano. The major advantage of using NCS group over CN is mainly on the lower rotational viscosity. The CN group has a larger dipole moment ( $\mu = 3.9$  D) than NCS ( $\mu = 3.7$  D) because of its linear structure. However, due to the very strong polarisation of the carbon–nitrogen triple bond the Huckel charges of carbon and nitrogen are high and well localised (22). Accordingly, dimers are formed by strong intermolecular interactions between the nitrile groups. Due to the longer  $\pi$ -electron conjugation, the NCS-based LC compounds exhibit

\*Corresponding author. Email: sgauza@mail.ucf.edu

a larger birefringence than the corresponding CN compounds. However, the NCS compounds tend to exhibit smectic phases (14). Because it is difficult to suppress the smectic phase without sacrificing the electro-optical performance of the LCs, here we investigate an intrinsic phenomenon of smectic-to-nematic (Sm–N) transitions.

In this paper, we present some high-birefringence single LC compounds exhibiting an enhanced figure-of-merit (FoM) when operated at a temperature near the Sm–N transition. The measured viscoelastic coefficient was significantly reduced near the Sm–N transition temperature resulting in  $\sim 75\%$  increase in FoM. Here, FoM is linked directly to the response time of the LC cell used for laser beam steering and light modulators: the higher the FoM, the faster the response time.

## 2. Experimental

Several techniques were used to measure the physical properties of the single compounds and mixtures. Differential scanning calorimetry (DSC, TA Instrument Model Q-100) was used to determine the phase transition temperatures. Results were obtained from 3–6 mg samples in the heating and cooling cycles at a  $2^\circ\text{C min}^{-1}$  scanning rate. The electro-optical properties of the LC compounds and mixtures were measured using  $5\ \mu\text{m}$  homogenous cells with indium tin oxide (ITO) electrodes coated in the inner sides of the glass substrates. A thin polyimide layer was overcoated on ITO and buffed in antiparallel directions to produce a small pretilt angle ( $\sim 2^\circ$ ). A linearly polarised He–Ne laser with  $\lambda = 633\ \text{nm}$  was used as the light source for the electro-optical measurements. Experimental setup and measurement technique were the same as those reported elsewhere (23).

The physical properties of the single compounds were measured at several temperatures within their nematic phase and results were used to fit with theoretical models. In this study, we focused on the birefringence ( $\Delta n$ ), viscoelastic coefficient ( $\gamma_1/K_{11}$ ) and figure-of-merit, which is defined as (24):

$$\text{FoM} = K_{11} \Delta n^2 / \gamma_1, \quad (1)$$

where  $K_{11}$  is the splay elastic constant and  $\gamma_1$  the rotational viscosity. The temperature-dependent birefringence of an LC can be described as follows:

$$\Delta n = \Delta n_o (1 - T/T_c)^\beta, \quad (2)$$

where  $\Delta n_o$  represents the birefringence at  $T = 0\ \text{K}$ ,  $\beta$  is a material constant and  $T_c$  is the clearing temperature of the LC. By fitting the experimental data using equation (2), we can obtain  $\Delta n_o$  and  $\beta$ . Once these two parameters are determined, the birefringence of the LC at room temperature can be extrapolated. Similarly we fit FoM with following equation (24):

$$\text{FoM} = a(\Delta n_o)^2 \left(1 - \frac{T}{T_c}\right)^{3\beta} \exp\left(\frac{-E}{\kappa T}\right), \quad (3)$$

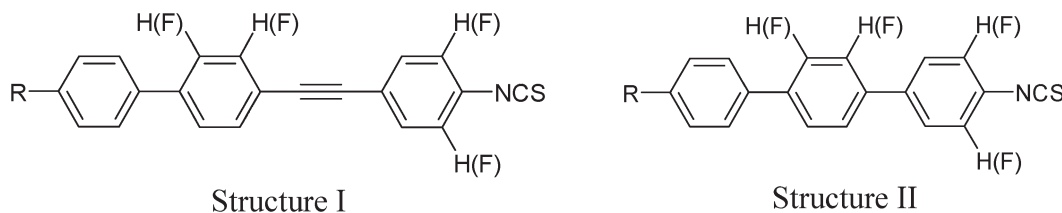
where  $a$  is a fitting parameter. The extrapolated viscoelastic coefficient at room temperature can be calculated from equation (1).

## 3. Results

Compounds with phenyl-tolane (structure I) and terphenyl (structure II) rigid cores were chosen for detailed investigation. Both structures exhibit a high optical anisotropy and are used for formulating high-birefringence mixtures. To widen the varieties we also synthesised compounds with different lateral fluorinations on the rigid cores (Scheme 1).

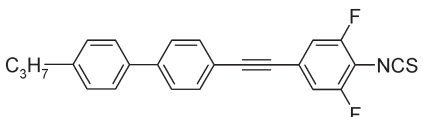
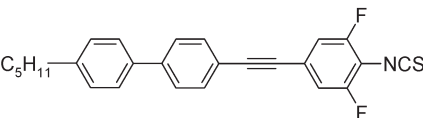
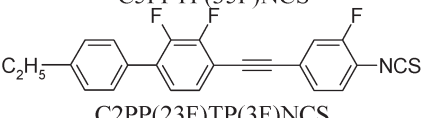
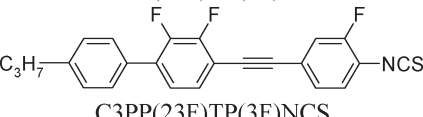
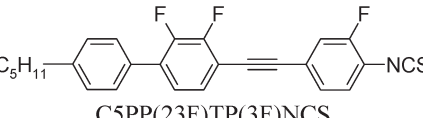
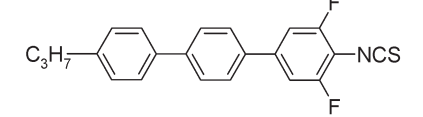
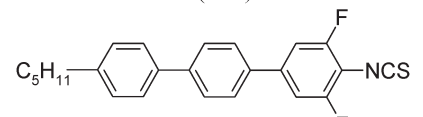
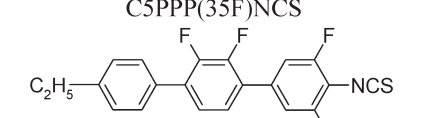
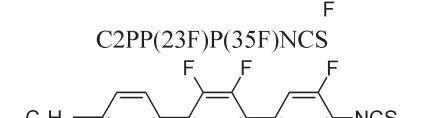
For isothiocyanates, homologues with a longer alkyl chain usually possess both smectic and nematic mesophases, whereas the shorter chain homologues tend to have only nematic phase.

Table 1 lists all the compounds included in the experiment with detailed molecular structures and phase transition temperatures. Also included for comparisons are two sets of fluorinated phenyl-tolanes (compounds **1a–1c** and **2a–2b**) and two pairs of fluorinated terphenyls (compounds **3a–3b** and **4a–4b**). The alkyl chain length was intentionally chosen



Scheme 1. Compounds with phenyl-tolane (structure I) and terphenyl (structure II) rigid cores.

Table 1. Single compound structures and phase transition temperatures.

ID No.	Structure	Phase transition temperatures /°C	$\Delta H$ (Cr-N)/cal mol <sup>-1</sup>
1a	 C3PPTP(35F)NCS	Cr 122.0 N 233.6 I	6263
1b	 C5PPTP(35F)NCS	Cr 55.0 S 119.0 N 208.5 I	3770
2a	 C2PP(23F)TP(3F)NCS	Cr 73.7 N 223.3 I	5452
2b	 C3PP(23F)TP(3F)NCS	Cr 82.2 S 89.2 N 240.5 I	5814
2c	 C5PP(23F)TP(3F)NCS	Cr 53.5 S 135.0 N 218.0 I	3359
3a	 C3PPP(35F)NCS	Cr 106.9 N 202.6 I	3359
3b	 C5PPP(35F)NCS	Cr 96.9 S 112.4 N 188.6 I	2174
4a	 C2PP(23F)P(35F)NCS	Cr 122.0 N 152.0 I	7040
4b	 C5PP(23F)P(35F)NCS	Cr 90.7 S 137.9 N 173.0 I	4089

to display different mesomorphic sequences within the compared sets. The difluoro-substituted isothiocyanato phenyl-tolane compounds **1a** and **1b** exhibit a wide nematic range with clearing temperature over 200°C. The propyl homologue shows a relatively high melting point (122°C). The pentyl homologue (compound **1b**) shows a much lower melting point temperature of 55°C, but smectic phase appears at

119°C. The fusion enthalpy ( $\Delta H$ ) is quite different for the C3 and C5 homologues. The  $\Delta H$  value (6.3 kcal mol<sup>-1</sup>) of compound **1a** is nearly twice as high as that of compound **1b**.

In the second series, we investigated different lateral fluorinations, as represented by compounds **2a**, **2b** and **2c**. Triple fluorination in this case was done by introducing fluorine into the second and

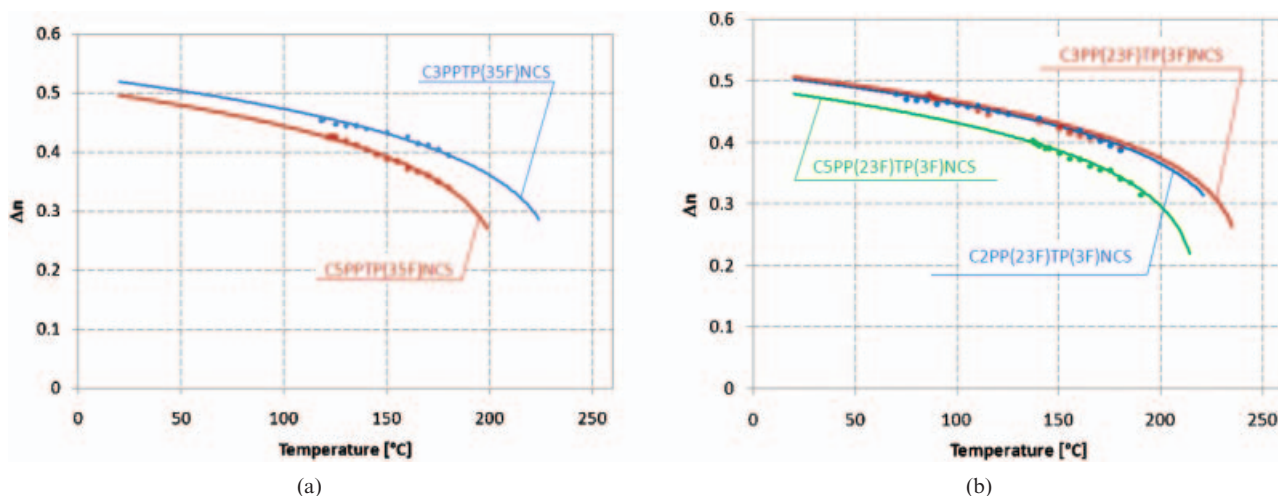


Figure 1. Temperature-dependent birefringence measured for (a) difluorinated phenyl-tolane isothiocyanates and (b) trifluorinated phenyl-tolane isothiocyanates.

third positions of the middle phenyl ring. The phenyl ring with a polar terminal group was single fluorinated at the position adjacent to the NCS terminal group. The measured melting temperature was significantly lower than the difluorinated compounds **1a** and **1b**. Only the ethyl homologue (C2) does not show a smectic phase; both propyl (C3) and butyl (C5) homologues exhibit a Sm–N transition at 89.2°C and 135.0°C, respectively. Also in this series, the pentyl homologue exhibits an exceptionally low  $\Delta H$  value (3.4 kcal mol<sup>-1</sup>). The presence of a smectic phase in the propyl and pentyl homologues was particularly attractive for investigating the Sm–N transition phenomenon. Similar to phenyl-tolane compounds, we intended to choose the same rigid core compounds but with different polymorphism. Compound **3a**, a short-chain homologue of the 3'',5''-difluoro-4''-isothiocyanato-4-alkyl-[1,1';4,1'']terphenyl series, exhibits only a nematic phase, whereas the pentyl homologue (compound **3b**) also possesses a smectic phase with transition to nematic at 96.9°C. A similar mesomorphic situation is observed for the ethyl (C2) and pentyl (C5) homologues of 2',3',3'',5''-tetrafluoro-4''-isothiocyanato-4-alkyl-[1,1';4,1'']terphenyl series. Compound **4a** with a shorter alkyl chain exhibits only a nematic phase, whereas compound **4b** with a longer chain exhibits both nematic and smectic phases. All the four sets reveal a lower melting temperature for the longer alkyl chain compounds, whereas smectic phase appears within the mesomorphic sequence. Compounds without a smectic phase have significantly higher melting temperatures. Therefore, their potential application for mixture formulations is limited because of their poor miscibility.

The measured temperature-dependent birefringence of these compounds follows the theoretical prediction by equation (3) regardless of their phases or mesomorphic sequence. Results are shown in Figure 1 for phenyl-tolanes and Figure 2 for terphenyl compounds. All phenyl-tolane compounds exhibit a birefringence slightly higher than 0.5 when  $\Delta n$  is extrapolated to the room temperature (~25°C). The only exception here is compound **2c**, for which  $\Delta n \sim 0.48$  under the same conditions. This can be explained on the basis of longest (C5) alkyl chain and triple lateral fluorination, which pulls electrons out of the conjugation within the rigid molecular core (25).

As for the terphenyl isothiocyanates investigated in our experiment, their birefringence is lower than that of phenyl-tolane compounds. This effect originates from the shorter conjugated rigid core as there is no carbon–carbon triple bond linking the terphenyl structure. Within the terphenyl series, the laterally difluorinated structures has a higher extrapolated birefringence ( $\Delta n \sim 0.45$  and 0.42, respectively, for compounds **3a** and **3b**) than their tetrafluorinated counterparts ( $\Delta n \sim 0.38$  and 0.35, respectively, for compounds **4a** and **4b**). Prior to determining the electro-optical performance of single compounds by calculating their figure-of-merit according to equation (1), we need to know the viscoelastic coefficient through the relaxation time measurements of a homogenous LC cell. As expected, the compounds with pure nematic phase (**1a**, **2a**, **3a** and **4a**) show exponential increase in viscoelastic coefficient as the temperature decreases. However, an abnormal behaviour near the phase transition boundary is found for the compounds with smectic–nematic sequence.



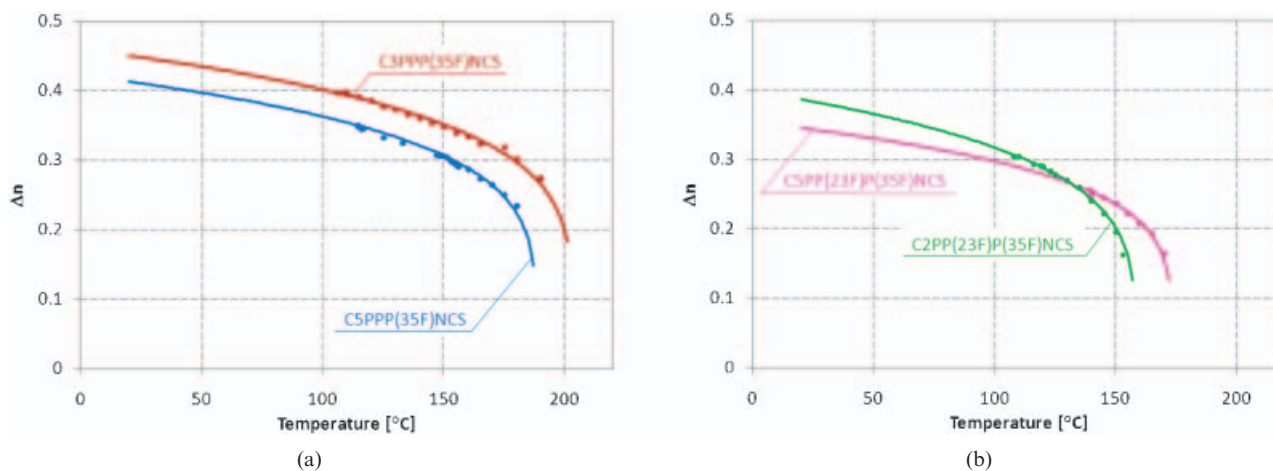


Figure 2. Temperature-dependent birefringence measured for (a) difluorinated terphenyl isothiocyanates and (b) trifluorinated terphenyl isothiocyanates.

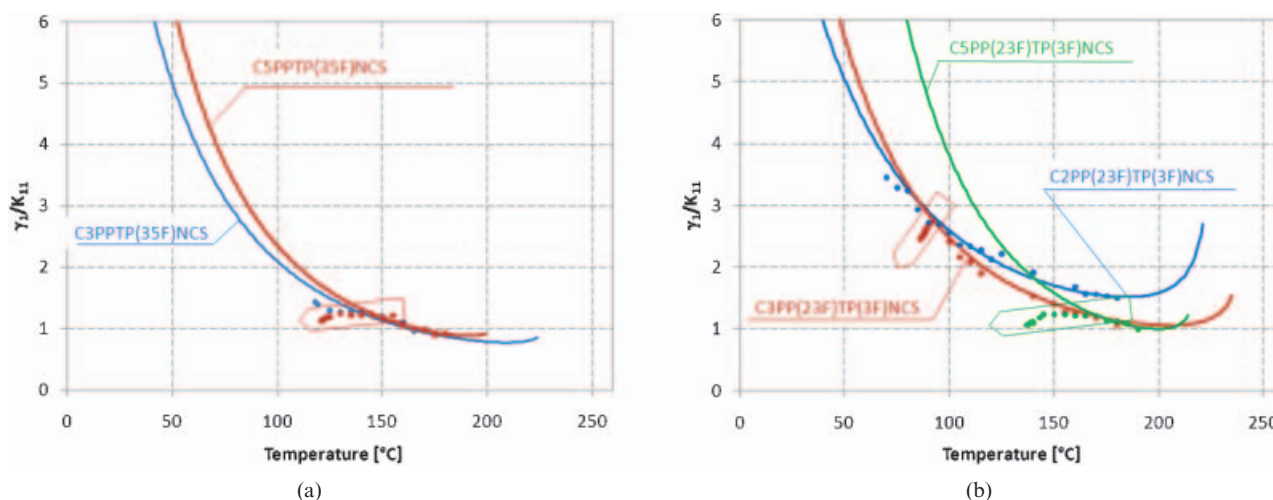


Figure 3. Temperature-dependent viscoelastic coefficient of (a) difluorinated phenyl-tolane isothiocyanates and (b) trifluorinated phenyl-tolane isothiocyanates.

Figure 3 shows the temperature-dependent viscoelastic coefficients of both phenyl-tolane sets. Here, we observed, obvious for compounds with smectic phase (**1b**, **2b** and **2c**), that the viscoelastic coefficient values resulting from relaxation time measurement do not follow the theoretical prediction at temperatures near the smectic to nematic transition. On the contrary, the viscoelastic coefficient decreases substantially as the temperature decreases, leading to a lower ( $\sim 33\%$ ,  $16\%$  and  $45\%$ )  $\gamma_1/K_{11}$  than the value expected from theoretical fitting at the same temperature for compounds **1b**, **2b** and **2c**, respectively. Similar behaviour was also observed for the terphenyl series. Compounds **3b** and **4b** exhibit a viscoelastic coefficient of about  $35\%$  and  $34\%$  from the one expected theoretically. Meanwhile, the viscoelastic coefficient of compounds **3a** and **4a** (without smectic phase) follows the theoretical prediction closely.

Figure 4 shows the detailed temperature-dependent viscoelastic coefficient data for both terphenyl pairs. A decreased viscoelastic coefficient was observed spanning over  $10\text{--}30^\circ\text{C}$ . A lower than predicted viscoelastic coefficient was observed within a wide temperature range for compounds **1b**, **2c** and **3b**. These compounds, regardless of the degree of fluorination, have the same long five-carbon alkyl chain.

Unexpectedly compound **4b**, which also has a pentyl chain, shows the discussed phenomenon only in a narrow temperature range, similar to short-alkyl chain compound **2b**. Consequently, the figure-of-merit calculated for the compounds with smectic-to-nematic phase transition is affected. In addition to decreased viscoelastic coefficient, birefringence slightly increases as the temperature decreases when the smectic–nematic transition temperature is approached from the nematic side. Both parameters

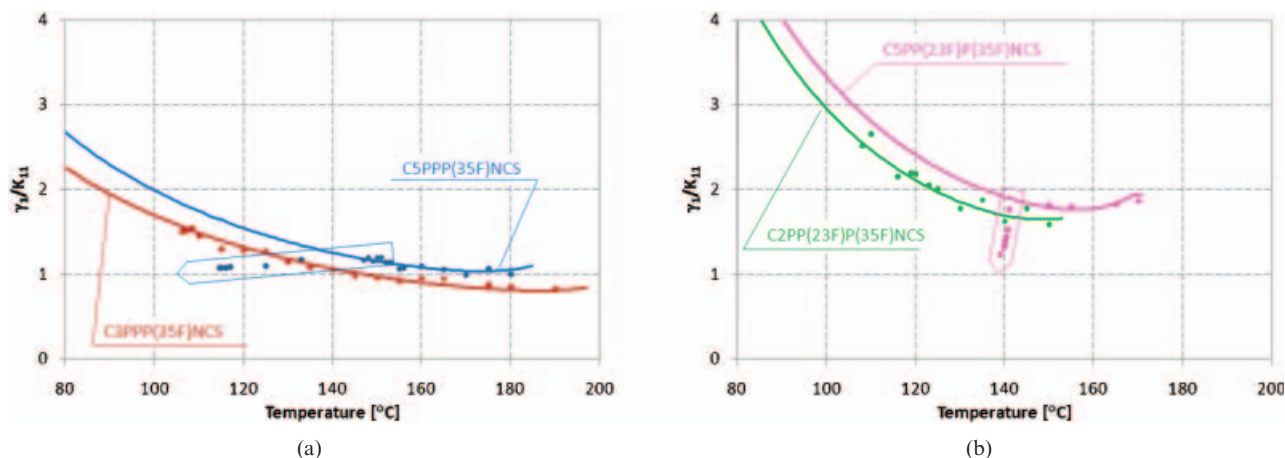


Figure 4. Temperature dependent viscoelastic coefficient of (a) difluorinated terphenyl isothiocyanates and (b) trifluorinated terphenyl isothiocyanates.

involved in FoM ( $\Delta n$  and  $\gamma_1/K_{11}$ ) change in the favourable directions, resulting in pronounced FoM near the smectic to nematic boundary. Phenyl-tolane compounds **1b**, **2b** and **2c** show a 75%, 32% and 38% higher FoM than their theoretically predicted values. In contrast, terphenyl compounds **3b** and **4b** show a 71% and 65% higher FoM than their theoretically predicted ones. Moreover, the FoM at vicinity of the Sm–N phase transition exceeds its maximum value at the optimal operating temperature by 23%, 44%, 39% and 33% for compounds **1b**, **2c**, **3b** and **4b**, respectively. An analogous situation does not take place in the case of terphenyl or phenyl-tolane compounds having only nematic liquid crystal phase. Figures 5–6 show the measured temperature-dependent FoM data for the phenyl-tolane and terphenyl series, respectively.

#### 4. Conclusion

The phenomenon of opposite change of viscoelastic coefficient reported here has been observed for the first time for high-birefringence terphenyl and phenyl-tolane isothiocyanates. Very detailed studies of flow viscosities, dielectric anisotropy and elastic constants of the cyanobiphenyl systems near smectic–nematic transitions are known for cyanobiphenyl-type liquid crystals and have been widely described and discussed by many authors (5–10). The conclusion of some of these experiments shows that at the temperatures slightly higher than the smectic-to-nematic transition there is a significant, but opposite to theoretical, change of the splay elastic constant  $K_{11}$ . At the same time, rotational viscosity remains rather unaffected (26). Comparison of our results on viscoelastic coefficient from measured optical relaxation time with the results for cyanobiphenyl

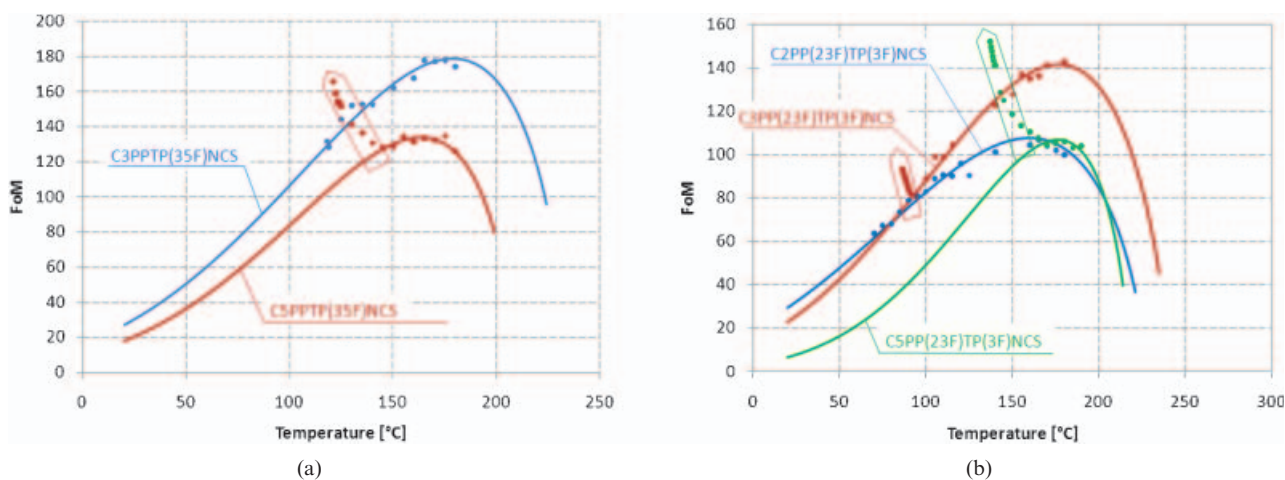


Figure 5. Temperature-dependent figure-of-merit of (a) difluorinated phenyl-tolane isothiocyanates and (b) trifluorinated phenyl-tolane isothiocyanates.

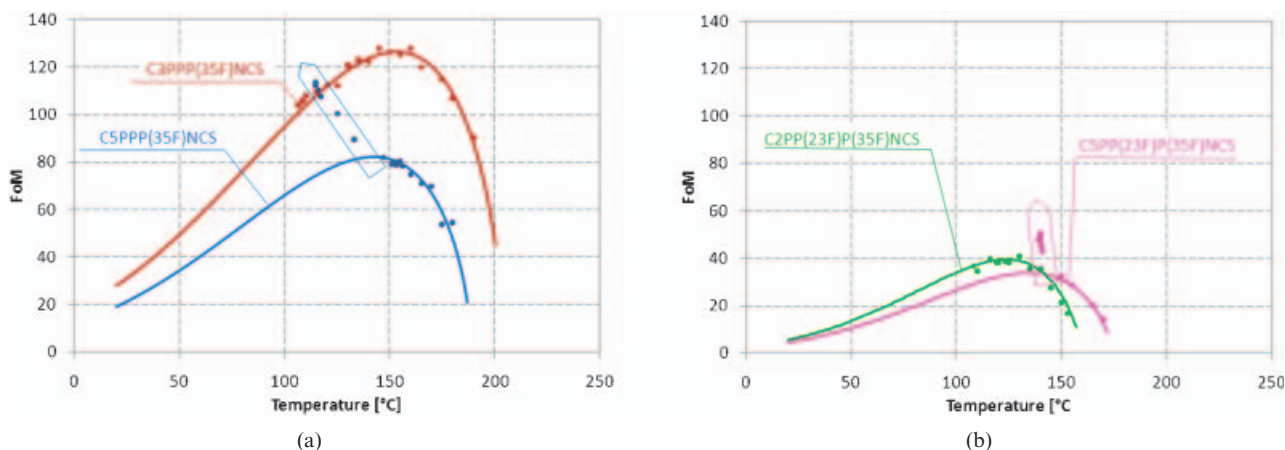


Figure 6. Temperature-dependent figure-of-merit of (a) difluorinated terphenyl isothiocyanates and (b) trifluorinated terphenyl isothiocyanates.

compounds shows good agreement. Investigation of isothiocyanato phenyl-tolanes and terphenyl compounds shows dramatic decrease of viscoelastic coefficient at the vicinity of a nematic-to-smectic phase transition. Typically, for the described phenyl-tolane and terphenyl isothiocyanates with smectic and nematic mesophases, the value of  $\gamma_1/K_{11}$  measured at the temperatures close to a phase transition corresponds to the value obtained at 10–40°C higher temperature. Moreover, the figure-of-merit achieves values higher than measured at the optimum operating temperature, according to equation(3). However, to utilise the observed phenomenon, the device temperature should be controlled within 1–4°C. We will continue to investigate application possibilities of these high-birefringence isothiocyanato phenyl-tolanes and terphenyl compounds and their mixtures. Mixtures, based entirely on laterally fluorinated phenyl-tolane isothiocyanates and terphenyl isothiocyanates are in the scope as initial high figure-of-merit and therefore short response time is expected (17). Although previously reported experiments indicates adequate thermal stability of similar materials (16, 27), the temperatures at which we operate single LCs for this experiment could be too high for reliable long-term operation. Therefore, new compound structures or mixtures for which the smectic to nematic transition temperature is close to the room temperature will be beneficial from the thermal stability viewpoint.

## References

- Gauza S.; Czupryński K.; Dąbrowski R.; Kenig K.; Kuczyński W.; Goc F. *Mol. Cryst. Liq. Cryst.* **2000**, *351*, 287–296.
- Gauza S.; Brodzik M.; Dąbrowski R.; Przedmojski J.; Ważyńska B. *Phase Transitions* **1997**, *60*, 223–237.
- Dąbrowski R.; Czupryński K.; Przedmojski J.; Wazynska B. *Liq. Cryst.* **1993**, *14*, 1359–1369.
- Kouwer P.H.J.; Pickenb S.J.; Mehl G.H. *J. Mater. Chem.* **2007**, *17*, 4196–4203.
- Yethiraj A.; Sun Z.; Dong R.Y.; Burnell E.E. *Chem. Phys. Lett.* **2004**, *398*, 517–521.
- Jadzyn J.; Czechowski G. *Phys. Rev. E* **2001**, *64*, 052702.
- de Jeu W.H.; Goossens W.J.A.; Bordewijk P. *J. Chem. Phys.* **1974**, *61*, 1985–1989.
- Cladis P.E. *Phys. Rev. Lett.* **1973**, *31*, 1200–1203.
- Jaishi B.R.; Mandal P.K. *Phase Transitions* **2005**, *78*, 569–592.
- DasGupta S.; Roy S.K. *Phys. Lett. A* **2003**, *306*, 235–242.
- Ramamoorthy A. (Eds), *Thermotropic Liquid Crystals: Recent Advances* **2007**. Springer: 2007, Chapter 8.
- de Vries A. *Mol. Cryst. Liq. Cryst.* **1970**, *10*, 219–236.
- Gauza S.; Wang H.; Wen C.H.; Wu S.T.; Seed A.; Dąbrowski R. *Jap. J. Appl. Phys., Pt. I* **2003**, *42*, 3463–3466.
- Spadło A.; Dąbrowski R.; Filipowicz M.; Stolarz Z.; Przedmojski J.; Gauza S.; Fan Y.H.; Wu S.T. *Liq. Cryst.* **2003**, *30*, 191–198.
- Gauza S.; Wen C.H.; Wu S.T.; Janarthanan N.; Hsu C.S. *Jap. J. Appl. Phys.* **2004**, *43*, 7634–7638.
- Gauza S.; Wen C.H.; Tan B.; Wu S.T. *Jap. J. Appl. Phys.* **2004**, *43*, 7176–7180.
- Gauza S.; Wen C.H.; Wu B.; Wu S.T.; Spadło A.; Dąbrowski R. *Liq. Cryst.* **2006**, *33*, 705–710.
- Gauza S.; Wu S.T.; Spadło A.; Dąbrowski R. *J. Display Technol.* **2006**, *2*, 247–253.
- Wu S.T.; Efron U. *Appl. Phys. Lett.* **1986**, *48*, 624–626.
- Gauza S.; Zhu X.; Wu S.T.; Piecek W.; Dąbrowski R. *J. Display Technol.* **2007**, *3*, 250–252.
- Jiao M.; Ge Z.; Song Q.; Wu S.T. *Appl. Phys. Lett.* **2008**, *92*, 061102–3.
- Huh I.K.; Kim Y.B. *Jap. J. Appl. Phys.* **2002**, *41*, 6484–6485.
- Wu S.T.; Efron U.; Hess L.D. *Appl. Opt.* **1984**, *23*, 3911–3915.
- Wu S.T.; Lackner A.M.; Efron U. *Appl. Opt.* **1987**, *26*, 3441–3445.
- Gauza S.; Parish A.; Wu S.T.; Spadło A.; Dąbrowski R. *Liq. Cryst.* **2008**, *35*, 483–488.
- DasGupta S.; Chattopadhyay P.; Roy S.K. *Phys. Rev. E* **2001**, *63*, 041703–8.
- Wen C.H.; Gauza S.; Wu S.T. *Liq. Cryst.* **2004**, *31*, 1479–1485.